water

MDPI

Review

Unraveling the "Black Box": Challenges and Perspectives in Elucidating Catalytic Mechanisms of Metal–Biomass Carbon Hybrids for Persulfate Activation

Jiahua Yu [1,2], Xiaoyang Chen [2,*], Lu Huang [2], Huangwei Chen [1,2] and Hengcong Tao [1]

[1] School of Petrochemical Engineering & Environment, Zhejiang Ocean University, Zhoushan 316022, China
[2] College of Environmental Science and Engineering, Zhejiang University of Water Resources and Electric Power, Hangzhou 310018, China
* Correspondence: chenxy@zuwe.edu.cn

Abstract

In recent years, Metal–Biomass Carbon (M–BC) hybrids have been widely studied as promising, cost-effective, and sustainable catalysts for persulfate activation in the degradation of emerging organic contaminants. M–BC systems offer advantages such as good performance and the sustainable use of biomass waste. Despite the considerable attention they have received, significant uncertainty remains regarding their precise catalytic mechanisms. A primary concern is the inherent complexity of biomass precursors, which frequently render the resulting catalytic structures ill-defined or akin to a "black box". To address this challenge, this review critically evaluates the current state of mechanistic research, focusing on the debate between radical and non-radical pathways. In this paper, five fundamental challenges to clear mechanistic understanding are identified, including interference of inherent inorganic species, lack of precursors standardization and inherent heterogeneity, ambiguous overlapping active sites, methodological limitations in chemical quenching due to competitive adsorption, and conductivity-related constraints on non-radical pathways. Among these, the interference from inherent inorganic species is of primary concern, as the available evidence suggests it frequently confounds reported synergistic effects. Additionally, the future research directions for improving the experimental standardization and mechanistic understanding of M–BC catalysts are proposed. This review enriches the field by providing a clear path toward rigorous mechanistic understanding and the rational design of M–BC catalysts for water remediation.

Keywords: metal–biochar composites; persulfate activation; emerging organic contaminants; catalytic mechanism

Check for updates

Academic Editor: Craig Allan

Received: 13 February 2026
Revised: 20 March 2026
Accepted: 27 March 2026
Published: 1 April 2026

Copyright: © 2026 by the authors. Licensee MDPI, Basel, Switzerland. This article is an open access article distributed under the terms and conditions of the Creative Commons Attribution (CC BY) license.

1. Introduction

Advanced Oxidation Processes (AOPs) generate powerful oxidizing radicals capable of completely mineralizing recalcitrant organic pollutants into harmless substances. However, their transition to large-scale application is frequently impeded by prohibitive operational costs linked to high energy and chemical consumption, harsh reaction conditions, and the critical risk of forming secondary oxidation by-products that may be more toxic than the original contaminants [1–3]. When comparing widely adopted catalytic AOPs, distinct operational trade-offs emerge: the homogeneous Fenton process offers rapid degradation with inexpensive reagents but is severely restricted by its narrow acidic pH requirement and massive iron sludge production. Conversely, semiconductor-based

photocatalysis avoids chemical sludge but is hampered by the high energy demands of UV light sources, reduced efficiency in turbid waters, and challenging catalyst recovery. To mitigate these inherent limitations, recent advancements have increasingly focused on designing novel emerging catalysts [4]. These catalysts include high-surface-area doped composites and zero-valent metals loaded on waste-derived supports, which are aimed at preventing electron-hole recombination, enabling operation at neutral pH, and eliminating sludge production [5,6]. The pursuit of high-performance catalytic materials has significantly propelled the development of sulfate radical-based advanced oxidation processes (SR-AOPs) for environmental remediation [7]. Relying on persulfate (including peroxymonosulfate (PMS) and peroxydisulfate (PDS)) for the in situ generation of sulfate radicals ($SO_4^{\bullet-}$), these systems have attracted widespread attention as more adaptable and cleaner alternatives to conventional treatment methods [8,9]. These processes not only overcome the dependence of traditional Fenton reactions on acidic pH but also demonstrate immense potential in degrading recalcitrant organic pollutants due to the long half-life and high oxidation potential of the radicals produced [10–12]. However, given the structural stability of the persulfate (PS) molecule, the release of its oxidative capability depends on an effective activation process [13]. Compared to physical activation methods (e.g., heat and UV) that are characterized by high energy consumption and complex equipment, chemical activation via transition metals is generally favored for its operational simplicity and high efficiency under mild conditions [7]. However, metal-based catalysts consistently face the challenge of secondary pollution during operation caused by the leaching of metal ions [14,15]. These challenges have driven interest in carbonaceous materials as green and stable, non-metal catalysts for AOPs [16,17]. Among these, crystalline carbon materials such as graphene and carbon nanotubes exhibit excellent performance, but their high synthesis costs limit scalable applications [18–20]. As a highly promising alternative, biomass carbon (BC) has garnered significant interest owing to its wide availability of precursors (e.g., agricultural waste), low cost, and the dual benefit of waste valorization (i.e., converting biomass waste into a functional material for water treatment) [21,22].

However, the practical application of pristine BC is constrained by its low graphitization degree and insufficient active sites [23]. To address these limitations, a common strategy involves the loading or encapsulation of metal species (e.g., Fe, Co, and Mn), leading to the formation of metal–biomass carbon (M–BC) hybrid materials [24]. In M–BC systems, the porous carbon matrix not only effectively disperses metal nanoparticles but also significantly inhibits metal ion leaching through the encapsulation effect of the carbon layer, thereby mitigating the secondary pollution problem and maintaining high catalytic activity [25,26]. Consequently, in recent years, M–BC hybrids have been widely studied as promising, cost-effective, and sustainable catalysts for persulfate activation in the degradation of emerging organic contaminants. As illustrated in Figure 1, the number of articles published on this matter per year shows a significant upward trend, reflecting a surge in research interest since 2019 that has remained highly active through recent years.

Despite the excellent performance of M–BC in pollutant degradation [27], the origins of this activity remain obscure due to the microscopic structure and active sites, resembling a "black box". Unlike structurally uniform synthetic nanocarbons, M–BC not only inherit the high compositional heterogeneity of biomass precursors (such as inherent N/S heteroatoms and inorganic ash) [28], but also involve intricate interactions among metal species, carbon defects, and oxygen-containing functional groups during the preparation process [29]. This structural and chemical complexity makes it challenging to identify the true active sites, resulting in considerable divergence in the literature regarding the underlying activation mechanisms.

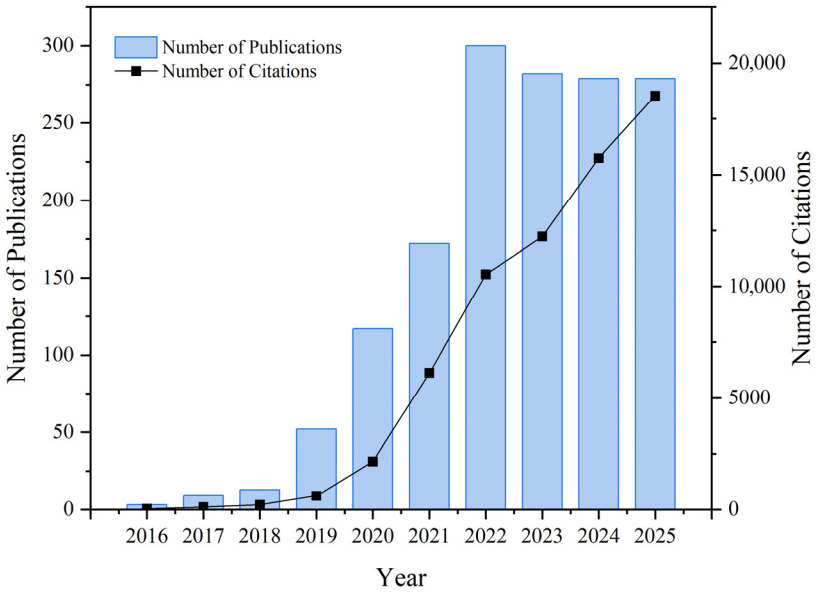


Figure 1. The publication trend of research articles related to M–BC hybrids for persulfate activation from 2016 to 2025. Data were retrieved from the Web of Science database.

Therefore, this review aims to critically evaluate the current understanding of the mechanisms underlying PS activation by M–BC. Specifically, it focuses on the challenges posed by the inherent compositional interference, precursor heterogeneity, and variable conductivity of BC in elucidating reaction pathways. Furthermore, perspectives are provided on how advanced characterization techniques may enable more precise delineation of the catalytic mechanisms in M–BC systems in the future. This review seeks to bridge the gap between mechanistic understanding and the practical application of biomass carbon catalysts, ultimately inspiring further innovations in this field.

2. Mechanisms of Persulfate Activation by M–BC

The catalytic nature of M–BC hybrid materials can be described as a "black box". Their overall catalytic activity does not arise from a mere additive effect of individual components, but rather from a synergistic interaction among the incorporated metal species, the biomass-derived carbon substrate, and the pyrolysis-generated metal–carbon interface. This structural complexity implies that the mechanism of PS activation is a result of the coexistence, competition, and even dynamic transformation of radical and non-radical pathways. This section systematically reviews these two fundamental pathways, particularly emphasizing how the biomass carbon substrate blurs the once-distinct boundaries between them, giving rise to significant challenges in mechanistic discrimination.

2.1. Radical Pathways

The radical pathway is the predominant oxidation mechanism in AOPs, relying on the generation of high-oxidation-potential $SO_4^{\bullet-}$ or $^{\bullet}OH$. In M–BC systems, the generation of these radicals is believed to originate from two major sources: Fenton-like reactions at metal sites and activation by defects/functional groups on the carbon substrate [30].

2.1.1. Fenton-like Reactions at Metal Sites

Transition metals (primarily Fe, Co, and Cu) incorporated into M–BC are widely regarded as the primary sites for generating radical species [31,32]. The mechanism conforms to classical Fenton-like reactions, where metal ions (e.g., Fe^{2+}, Co^{2+}) cleave the O–O

peroxide bond of persulfate through single-electron transfer [33,34]. This is exemplified by the activation of PMS (HSO_5^-) and PDS ($S_2O_8^{2-}$), as shown in Figure 2a:

$$M^{n+} + HSO_5^- \rightarrow M^{(n+1)+} + SO_4^{\bullet-} + OH^- \text{ (PMS activation)}$$

$$M^{n+} + S_2O_8^{2-} \rightarrow M^{(n+1)+} + SO_4^{\bullet-} + SO_4^{2-} \text{ (PDS activation)}$$

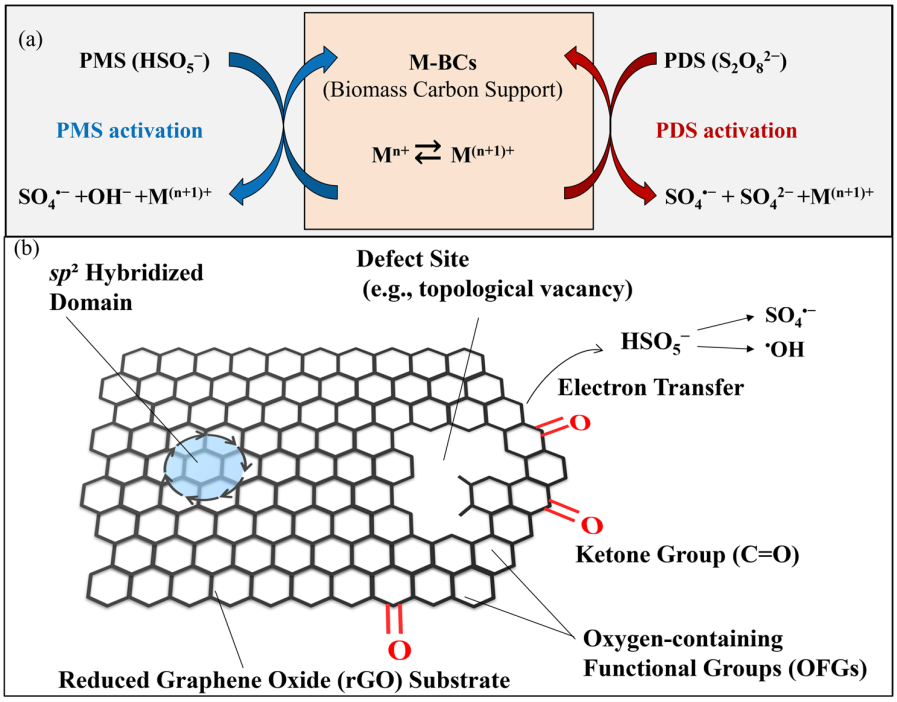


Figure 2. (**a**) Schematic diagram of the M–BC activation of PS. (**b**) Mechanism of PMS activation by intrinsic carbon defects and functional groups.

In this initial cleavage step, the metal center acts as an electron donor and is oxidized to $M^{(n+1)+}$. Because the active site is not regenerated, it acts merely as a stoichiometric reactant. To close the catalytic cycle, the oxidized metal must be subsequently reduced back to its initial state (e.g., $M^{(n+1)+} + HSO_5^- \rightarrow M^{n+} + SO_5^{\bullet-} + H^+$) [7,35]. In M–BC systems, the biochar support plays a critical role in this regeneration step. The conductive carbon matrix can act as an electron shuttle, facilitating the transfer of electrons from adsorbed organic pollutants directly to the oxidized metal centers [36]. This synergy accelerates the thermodynamically rate-limiting reduction of $M^{(n+1)+}$ back to $M^{(n)+}$, thereby sustaining the catalytic cycle and preventing the reaction from stalling as an ordinary stoichiometric oxidation [7].

Within such heterogeneous catalytic processes, recent studies emphasize the critical role of surface-bound radicals. In M–BC systems, a significant portion of the generated reactive species does not diffuse away immediately. Instead, they remain coordinated to the active sites, forming highly reactive surface-bound radicals. These surface-confined species efficiently degrade pollutants that are pre-adsorbed on the catalyst surface, avoiding the severe quenching effects typically observed in bulk solutions [37–39].

In this conventional perspective, the BC carrier is frequently perceived as a largely inert scaffold. Its core functions are: (1) to achieve efficient dispersion of metal nanoparticles through its porous structure, exposing more active sites [40]; and (2) to anchor metal species through carbon layer encapsulation or carbon–metal coordination, thereby inhibiting metal ion leaching and mitigating the secondary pollution issue of traditional homogeneous cata-

lysts [41]. However, this simplified view of M–BC merely as "supported Fenton catalysts" significantly underestimates the complexity and active role of the carbon substrate itself.

2.1.2. Defects and Functional Groups on Carbon Substrate

In contrast to highly graphitic crystalline carbons, BC is far from an inert carrier. The pyrolysis process inherently introduces a high density of structural defects into the carbon skeleton, which fundamentally alters the local electron distribution and creates highly reactive centers. Specifically, topological defects disrupt the structural symmetry of the carbon lattice, exposing localized unpaired electrons on dangling bonds that facilitate direct electron transfer to persulfate molecules [42,43]. Similarly, compared to pristine basal plane carbons, edge sites (particularly those in zigzag configurations) possess higher localized spin densities and stronger adsorption affinities for persulfate molecules [44,45]. Furthermore, heteroatom doping inherent to many biochars introduces active sites such as graphitic (or quaternary) nitrogen. Drawing on mechanisms observed in nanocarbons, the incorporation of highly electronegative nitrogen atoms into the sp^2-hybridized carbon framework withdraws electrons from the conjugated π-system. This electron transfer imparts a substantially high positive charge density on the adjacent carbon atoms, generating highly active catalytic centers [46,47]. These electron-deficient carbon sites exhibit an enhanced affinity for nucleophilic attack by persulfate anions, where the subsequent electron delivery from the anions to the carbon matrix triggers the oxidation of persulfate into singlet oxygen [48]. Alongside these structural and doping-induced defects, abundant surface functional groups (especially carbonyl C=O, quinone groups, and other oxygen-containing functional groups) [49,50]. Intrinsic features such as sp^2 hybridized domains, defects, and carbonyl groups are widely recognized as active sites. These moieties can function as electron donors or activation centers, directly triggering persulfate decomposition and radical generation [51,52]. For instance, analogous to studies on reduced graphene oxide (rGO), ketone groups (C=O) have been identified as key active sites capable of triggering PMS decomposition via electron transfer, thereby efficiently generating $SO_4^{\bullet-}$ and $^{\bullet}OH$ (Figure 2b).

Crucially, for these intrinsic carbon sites to operate catalytically rather than as stoichiometric reductants, they must return to their original state after activating the persulfate. Once functional groups or defect sites donate electrons to cleave the peroxide bond, they enter an oxidized state [53]. To close the catalytic loop, these electron-depleted sites continuously abstract electrons from the targeted organic pollutants [38]. The extensive π-conjugated network of the biochar ensures rapid electron mobility, allowing the carbon substrate to simultaneously oxidize the pollutant and regenerate its own active sites [53].

However, it is crucial to emphasize that the probability of activation mechanisms driven by oxygen-containing groups is highly dependent on the preparation methods of the biochar and its derivatives. As different synthesis routes lead to fundamentally distinct surface properties, the contribution of this specific pathway varies significantly [54,55]. Biochars produced at relatively low temperatures or subjected to chemical oxidation exhibit rich surface oxygen functionality, making this pathway highly probable. Conversely, at high pyrolysis temperatures (e.g., >700 °C) and under controlled inert atmospheres, oxygen-containing groups largely decompose and volatilize [56–58]. Under such conditions, the probability of oxygen-functional-group-mediated activation is drastically reduced, and the dominant intrinsic carbon activation mechanism shifts almost entirely toward the aforementioned topological defects, edge sites, and graphitic structures [59].

Consequently, a key complexity in M–BC systems is distinguishing whether the observed radical generation stems from a genuine synergy between the metal and the carbon, or merely represents an additive effect of their independent contributions. This

intrinsic catalytic "background" from the carbon substrate thus represents the foremost challenge in precisely elucidating the activation mechanism of M–BC.

2.2. Non-Radical Pathways

In recent years, the research paradigm has gradually shifted from traditional radical-dominated pathways to non-radical pathways. In numerous M–BC systems, non-radical pathways have been demonstrated to play a dominant role [60,61]. For example, Nguyen et al. confirmed that in the degradation of antibiotics using nickel ferrite/biochar composites (DP–BC@$NiFe_2O_4$), the dominant reactive species was not radicals but singlet oxygen ($^1O_2$) [62]. Unlike radicals that attack indiscriminately in the bulk solution, non–radical oxidation processes mainly occur at the catalyst–solution interface, thus typically exhibiting stronger anti-interference capability against complex water environments (e.g., high concentrations of chloride ions, natural organic matter) and higher reaction selectivity [63].

Based on current understanding, the non-radical mechanisms of PS activation by M–BC are primarily categorized into three types: $^1O_2$ generation, direct electron transfer (DET), and the formation of surface-activated complexes [64–67].

2.2.1. $^1O_2$ Pathway

$^1O_2$ is an electrophilic reactive species with high selectivity, tending to preferentially oxidize electron-rich compounds (such as phenols, amines, and specific antibiotics) [68]. In carbon-based catalytic systems, the generation of $^1O_2$ is closely related to oxygen-containing functional groups on the material surface [69]. A prevalent mechanism is that ketone/carbonyl groups at the edges of the carbon material act as nucleophilic sites, interacting with PMS molecules through a nucleophilic addition mechanism to form a metastable dioxirane intermediate, which subsequently decomposes to release $^1O_2$ [65,70].

Since biomass carbon (especially samples prepared via medium-to-low temperature pyrolysis) is inherently abundant in such oxygen-containing groups, the $^1O_2$ pathway is particularly common in M–BC systems. For example, Bao et al. reported that biochar pyrolyzed at 450 °C possessed a high density of C=O and C–OH sites [71]. The significant consumption of these groups post-reaction showed a positive correlation with $^1O_2$ production. This phenomenon indicates that medium-to-low temperature biochar, by virtue of its rich surface chemistry, has a natural tendency to induce non-radical pathways.

2.2.2. DET Pathway

DET represents a distinct activation mechanism independent of reactive oxygen species generation. In this pathway, M–BC functions as an electron shuttle or conductive bridge [36]. The core process includes: (1) simultaneous adsorption of the pollutant (electron donor) and persulfate (electron acceptor) onto the catalyst surface; and (2) direct transfer of electrons from the pollutant to the persulfate through the highly conductive carbon substrate, resulting in the direct oxidative decomposition of the pollutant [66,72]. According to Miao et al., the intrinsic defects in biochar play a pivotal role in the non-radical activation of PDS. These defects induce electron redistribution and form partially positive carbon atoms, which serve as active sites for PDS adsorption. The study proposes that these defects act as electron mediators, facilitating electron transfer from contaminants to the adsorbed PDS (forming metastable BC–PDS species) and reducing the HOMO–LUMO gap, thereby driving the non-radical oxidation process.

The efficiency of the DET pathway is strongly governed by the material's conductivity and degree of graphitization. In M–BC systems, loaded metals (particularly Fe, Co, and Ni) can significantly catalyze the transformation of amorphous carbon to graphitic carbon during pyrolysis [73]. Therefore, the DET pathway is often used to explain the high

catalytic activity of M–BC that are prepared at high temperatures and possess developed graphitic networks.

2.2.3. Surface-Activated Complex Pathway

This pathway represents a hybrid mechanism that bridges radical and non-radical processes. The mechanism proposes that the PS is adsorbed onto catalyst active sites (e.g., metal centers or carbon defects) without cleaving its peroxide bond to generate free radicals. Instead, it forms a metastable, high-oxidation-potential surface-activated complex [74]. Although this surface complex does not release "free-moving" $SO_4^{\bullet -}$ into the solution, it can directly oxidize pollutant molecules adsorbed on adjacent sites [75]. Some studies also describe this as "surface-bound radicals", implying that the radicals are confined within the electrical double layer and are restricted from diffusion [67]. The existence of this mechanism further complicates the "black box" characteristic of M–BC. It renders traditional chemical quenching experiments (such as using macromolecular humic acid or alcohols) highly unreliable, as quenchers are often unable to access these active species bound to the surface due to steric hindrance [53,76].

2.3. Complexity and Interplay of Mechanisms

While the theoretical delineation between radical and non–radical pathways appears distinct, these boundaries blur significantly in actual M–BC systems. Crucially, this blurring is driven by profound synergistic interactions between the metal sites and the biochar matrix, rather than mere physical mixing. The chemical bonding between the metal and biochar fundamentally alters the electronic structure of the metal's active site [77,78]. Biochar, with its rich π-conjugated carbon network and functional groups, often acts as an electron shuttle [79]. This electron transfer process increases the electron density around the metal center, thereby directly modulating its catalytic properties. Consequently, the activation energy required for the rate-determining step in persulfate activation—typically the reduction of high-valence metal species—is significantly lowered [80,81]. This electronic modulation accelerates the redox cycling of the metal, boosting the generation of reactive oxygen species via the radical pathway. Furthermore, the electron-enriched metal–carbon interfaces can optimize the adsorption energy of persulfate, favoring the formation of surface-activated complexes and facilitating DET or $^1O_2$ generation via non-radical pathways [82–84].

Unlike structurally uniform nanocarbons, M–BC possess a heterogeneous biomass origin. Metal sites, carbon defects, oxygen functionalities, and heteroatoms overlap extensively at the microscopic scale, leading to the simultaneous occurrence and competition of multiple pathways. This inherent complexity creates a fundamental disconnect between theory and experimental verification. The coexistence of varying mechanisms renders the contributions of individual pathways difficult to decouple using conventional means. For instance, determining whether the degradation is driven by specific metal active sites or adjacent carbon defects remains a formidable task.

Consequently, the field faces considerable challenges in accurately attributing catalytic activity to specific mechanisms. The unique "in–situ hybrid characteristics" of M–BC impose methodological hurdles that traditional catalytic models struggle to resolve. The following section (Section 3) will systematically address these impediments—specifically the interference of indigenous impurities, the ambiguity of active sites, and the limitations of scavenging assays—to elucidate why a definitive mechanistic understanding of M–BC systems remains elusive.

3. Unique Challenges in M–BC Mechanistic Research

M–BC systems theoretically possess both radical and non-radical pathways simultaneously. Moreover, in practice, accurately identifying which pathway dominates and attributing it to specific active sites is extremely difficult. This is primarily because M–BC present a series of unique challenges distinct from crystalline carbons (e.g., graphene and CNTs) [85].

As demonstrated in Table 1, despite the aforementioned mechanistic challenges, M–BC systems have been broadly applied in various environmental remediation scenarios. These functionalized biochars exhibit exceptional performance in degrading a wide spectrum of emerging contaminants, including antibiotics and industrial organic pollutants in complex water matrices. Their robust catalytic activity makes them highly promising for practical applications such as aquatic ecosystem remediation and pharmaceutical wastewater treatment. However, precisely decoupling the radical and non-radical contributions remains essential for the targeted design of M–BC catalysts tailored to specific environmental applications.

Table 1. Comparison of recent M–BC systems: Target applications, dominant pathways, and identification methods.

M–BC Catalyst	Oxidant	Contaminant	Application	Dominant Pathway	Identification Method	Ref.
CSBC	Fe (VI)	Sulfamethoxazole	Water purification	Radical ($^{\bullet}O^{2-}$) and Non-radical	Quenching tests, Electron paramagnetic resonance (EPR), DFT	[86]
G-nZVI-BC	PDS	*p*-Nitrophenol	Water treatment	Radical (key role) and Non-radical	Quenching tests, EPR	[30]
FC@N-BC	H_2O_2	Tetracycline	Antibiotic removal	Radical ($^{\bullet}OH$ dominant)	Quenching tests, EPR	[31]
E-Co/SBC@NF	PMS	Sulfamethoxazole	Aquatic ecosystem remediation	Radical and Non-radical (Combined)	Quenching tests, DFT	[32]
Fe-O-BC	PMS	Tetracycline	Pharmaceutical wastewater treatment	Radical ($^{\bullet}OH$, $SO_4^{\bullet-}$ dominant)	Scavenging experiments	[33]
GBC-1000	PDS	Tetracycline	Environmental remediation	Non-radical (Electron transfer)	EPR, In situ Raman, LSV, electrochemical impedance spectroscopy (EIS)	[66]

3.1. Interference from Inherent Components

In the field of M–BC catalysis, a standard experimental design involves comparing "metal-loaded biomass carbon" (M–BC, experimental group) with "pristine biomass carbon" (BC, control group) to isolate and demonstrate the contribution of the intentionally loaded metal [86,87]. A fundamental flaw in this design, however, lies in its underlying assumption that pristine BC is an inert and chemically "clean" substrate. This assumption is particularly problematic when the biomass originates from waste.

Specifically, biomass precursors, especially sludge, animal manure, or food waste, contain inherently significant amounts of inorganic ash [88]. This ash does not disappear

during pyrolysis but is concentrated and transformed into inorganic mineral phases, among which are potentially catalytically active substances. For instance, municipal sludge is recognized as a feedstock rich in Fe, Al, Ca, and Mg, with an ash content that can reach 20–40% [89]. Similarly, animal manure contains substantial levels of mineral elements, including K, P, Ca, Mg, and Fe [90]. During pyrolysis, these inherent Fe, Ca, and Mg are likely to transform into catalytically active oxides such as Fe_3O_4, CaO, and MgO [91,92]. Indeed, interference from such inherent activity is frequently observed in the literature. Numerous studies report that "pristine" sludge carbon, without any additionally loaded metal, exhibits strong activation capability for PS [93,94]. However, these studies often vaguely attribute this activity to "carbon defects" or "oxygen-containing functional groups", while systematically neglecting the catalytic contribution of inherent metal species like Fe/Ca/Mg within its high ash content.

Consequently, a core methodological challenge in evaluating loaded M–BC is how to establish a genuinely valid blank control. Many studies employ pristine biochar as a control, but the adequacy of this reference material is critically dependent on the nature of its precursor feedstock.

In the case of relatively "clean" feedstocks such as lignocellulose, the opposite scenario holds true. Pristine biochar prepared from such feedstocks is typically considered a substrate with limited function. As noted in a review, the functionality of pristine biochar is often limited by its scarcity of surface functional groups, frequently necessitating modification via methods such as metal loading [94]. Experimental evidence supports this view. A study on beech wood biochar found that the degradation efficiency of "clean" biochar (without added mineral ash) was significantly lower than that of its ash-amended counterpart [95]. Therefore, such "clean" pristine biochar has extremely low catalytic activity and can be regarded as an effective blank control for evaluating the contribution of loaded metals.

In contrast, once mineral-rich feedstocks like sewage sludge are used, "pristine biochar" itself becomes an efficient catalyst. This severely interferes with the assessment of the catalytic contribution of "loaded" metals. For example, Kanafin et al. confirmed that "pristine" sewage sludge biochar (without extra loading) possessed strong PS activation capability, primarily attributed to surface-bound inherent Fe and Al species [92]. Consequently, in M–BC research, the feedstock origin of the pristine biochar control must be rigorously scrutinized. If a study uses metal-rich pristine carbon (like sludge carbon) as a control, its conclusions regarding the "contribution of loaded metals" are likely to contain systematic bias. To eliminate this bias and establish a catalytically inert baseline for mineral-rich feedstocks, an acid-washing pretreatment is typically required. This demineralization process effectively leaches out inherent metal species, minimizing the background catalytic interference from intrinsic ash [96,97]. Therefore, to accurately assess the catalytic contribution of intentionally loaded metals on waste-derived substrates, the M–BC should be compared against acid-washed biochar instead of pristine biochar. This approach ensures a rigorous and reliable experimental design [98,99].

3.2. Heterogeneity of Precursors

Unlike the well-defined catalytic patterns of crystalline carbons, which are derived from highly standardized industrial products, M–BC systems face a fundamentally different challenge. This complexity is rooted in the intrinsic heterogeneity of biomass-derived carbon (Figure 3). Even feedstocks of the same nominal type exhibit substantial inherent variability in composition and structure. The chemical composition, physical structure, and consequently the catalytic pathways of the resulting biochar are profoundly dependent on the precursor source.

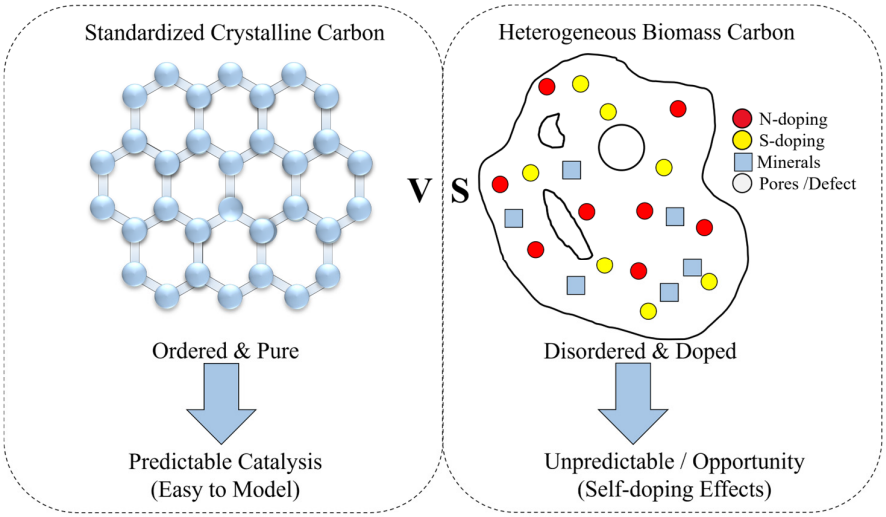


Figure 3. Schematic comparison between standardized crystalline carbon and heterogeneous biomass carbon.

This Profound dependence on precursors leads to a significant lack of standardization. For example, biochar produced from different waste parts of the same pecan plant exhibited significant differences in key chemical compositions and physical structures, such as mineral content, fixed carbon, and pH [100]. When this microscopic heterogeneity extends to macroscopic industrial applications, the challenge becomes even more severe [101]. In discussing the use of municipal solid waste (MSW) as a precursor, it was explicitly stated that the "dense and amalgamated nature" of the feedstock is a direct "challenge" for scalable production. Thus, this inherent heterogeneity derived from precursors not only makes the performance of M–BC catalysts difficult to precisely predict and reproduce across laboratories but also constitutes a massive obstacle to their industrial and scalable application.

While heterogeneity poses significant challenges, it concurrently presents unique opportunities. Utilizing these precursors rich in specific elements for in situ self-doping has emerged as a key in the M–BC field. When researchers use sludge, animal manure, or other heteroatom-rich biomass (such as pea peels and other agricultural wastes) as precursors, they find that this "natural N, S co–doping" [102] can greatly promote catalytic activity. The resulting performance surpasses not only that of undoped carbons but also materials doped with only a single heteroatom. A comparative study demonstrated the synergistic effect of N, S co-doping, which simultaneously improves the density of active sites and enhances conductivity [103]. Mechanistically, as noted in the review by Gao et al., the introduction of heteroatoms (especially N) breaks the inertness of traditional carbon materials; it effectively "regulates its electronic properties" and "induces more active sites" on the carbon skeleton [104]. Therefore, the reconstruction of the electronic structure triggered by precursor-derived N, S doping is considered a key prerequisite for forming highly active M–N–C or M–S–C synergistic sites. These synergistic sites can more effectively adsorb and activate reactants (such as persulfate or oxygen), thereby greatly promoting the generation of reactive oxygen species (ROS) and ultimately enhancing catalytic performance.

In addition, the real challenge lies in the fact that when we attempt to generalize the "N, S doping" principles derived from "heteroatom–rich" precursors (like sludge or manure) to lignocellulosic precursors (like sawdust or straw) traditionally considered to have extremely low N/S content, the challenges of lack of standardization and inherent heterogeneity in the M–BC field become even more intractable. A common assumption is

that M–BC derived from such "clean" feedstocks, presumably lacking N/S doping sites, would follow mechanistic models centered on physical adsorption (via pore structure) or reactions mediated by oxygen-containing functional groups. However, in-depth studies have revealed a deeper issue of a lack of standardization [105,106].

Specifically, these two papers challenge the simple assumption of "lignocellulose = no N doping." Although Fang et al. [105] used pine sawdust and Xu et al. [106] used bamboo leaves—neither being nitrogen-rich precursors—both studies confirmed the existence of active N doping sites (pyridinic N, pyrrolic N, etc.) via XPS and explicitly stated that these M–N–C sites were key to PMS activation. Moreover, even after confirming the presence of similar M–N–C sites, the two studies arrived at diametrically opposed conclusions regarding the dominant catalytic pathway.

This difference in mechanism corroborates the view at the beginning of this section: the lack of standardization and inherent heterogeneity of biomass carbon lead to extreme unpredictability in catalytic behavior. Even with the same type of biomass, widely divergent mechanistic models can arise across different laboratories and metal loading systems. This absence of structure–activity relationships and mechanistic confusion is the greatest obstacle hindering the cross-laboratory reproduction and industrial application of M–BC technology.

3.3. Ambiguity of Active Sites

M–BCs constitute complex, heterogeneous catalytic systems often described as "black boxes". This complexity largely originates from the diversity of strategies used to convert biomass into a catalytic support. Unlike relatively clear systems like cobalt-loaded graphene, the potential active sites of M–BC are highly overlapping and coexistent [107–109]. These sites include at least: (1) loaded metals (e.g., Fe, Co) [110]; (2) oxygen-containing functional groups on the carbon carrier (e.g., C=O, –OH) [111]; (3) carbon defects/edge structures [112]; and (4) heteroatom doping sites like N, S [113]. In M–BC, these sites are highly interwoven, making mechanistic attribution extremely challenging.

In M–BC catalytic systems, a long-debated core "discrepancy" exists regarding the catalytic mechanism. On the one hand, extensive literature [114,115] attributes the efficient catalytic activity to Fenton-like radical processes dominated by metal sites (whether Fe/Co clusters or Fe single atoms), generating ROS such as $^{\bullet}OH$ and $SO_4^{\bullet-}$ via redox cycles like Fe(II)/Fe(III). In this view, the BC is often regarded as a largely inert carrier. On the other hand, abundant literature also points out that metal-free biomass carbon itself is not inert; its rich quinone functional groups serve as redox active centers capable of degrading pollutants via non-radical pathways (e.g., inducing $^1O_2$ production through nucleophilic attack) [116,117].

This duality raises a critical question: in M–BC systems possessing both types of active sites (metal centers and carbon-based functional groups), do these two pathways operate in coordination, in competition, or have they been confused in previous studies? Recent research offers an elegant answer to this "contradiction" [118]. The study indicates that these two pathways (metal-radical vs. carbon-non-radical) coexist and compete. More importantly, the system exhibits a substrate-dependent selective-adsorption mechanism. The properties of the pollutant—notably its ionization potential (IP)—determine its preferred adsorption site. For instance, low-IP pollutants (e.g., bisphenol A) tend to occupy Fe clusters, thereby inhibiting the radical pathway and forcing the system to switch to efficient electron transfer processes at other sites, such as Fe single atoms. In contrast, high-IP pollutants (e.g., nitrobenzene) may preferentially adsorb at Fe single-atom sites, leaving Fe clusters available to freely generate radicals via Fenton-like reactions. Thus, the "contradictory" phenomena reported in the literature may not be apparent inconsistency,

but rather a precise, switchable catalytic selectivity inherent to the Fe–BC system that depends on substrate (pollutant) properties.

3.4. Limitations of Quenching Experiments

Despite recent advances in mechanistic understanding, research on M–BC continues to be constrained by an inherent methodological limitation in verifying radical-based pathways. Currently, the predominant approach for mechanistic investigation primarily relies on chemical quenching experiments (e.g., using TBA and MeOH) [119,120]. However, the validity of this approach is significantly confounded when applied to high surface area, porous adsorbents like M–BC due to complex interfacial behaviors [103].

In heterogeneous systems like M–BC, quenching agents do not act exclusively as bulk-phase radical scavengers. They also partition and adsorb onto the catalyst–solution interface, driven by their physicochemical properties such as hydrophobicity [121]. Consequently, when both the quencher and the target pollutant adsorb onto the interface, they engage in direct competition for active sites and surface-bound radicals [122–124]. This leads to a significant confounding effect, where the apparent inhibition observed may stem from competitive site blocking rather than from genuine chemical quenching of radicals, making the two effects practically indistinguishable.

Therefore, this inability to decouple physical blocking from chemical scavenging renders many historical mechanistic conclusions subject to re-evaluation [125]. The over-reliance on quenching experiments—without correcting for adsorption artifacts—implies that many reported mechanisms, particularly those attributing performance enhancements to specific "synergistic effects," may lack robust empirical verification rather than empirically proven [125,126].

3.5. Conductivity Limitations on Non-Radical Pathways

The DET pathway is a critical component of non-radical mechanisms in carbon materials, relying on the material to serve as an "electron bridge" for efficient conduction [53,127,128]. While crystalline carbons excel in this role due to their superior conductivity, biomass carbon is inherently limited [129]. Extensive research indicates that biochar prepared at medium-to-low temperatures (e.g., 400–700 °C) exhibits extremely negligible conductivity, often displaying semiconductor or even insulator characteristics. This fundamental physical property severely restricts the feasibility of the DET pathway in these materials.

This conductivity deficit stems from the insufficient graphitization of biomass within this temperature range. As demonstrated by Antic Gorrazzi et al., BC prepared at 500 °C (E500) remains dominated by amorphous, disordered carbon structures. This structural state results in a pronounced disparity in conductivity: E500 exhibits a conductivity of only 10^{-6} S/cm, and even at 600 °C, it remains limited to 10^{-4} S/cm—nearly a million times lower than graphite (~100 S/cm) [130]. Functionally, this manifests as a prohibitive potential drop; for instance, E500 creates a 1.2 V drop that renders the surface potential unfavorable for bacterial respiration, whereas the drop for E1000 is negligible (0.4 mV). Consequently, the physical properties of medium-to-low temperature biochar render it incapable of effectively sustaining the electron flux required for DET (Figure 4).

The structural origin of this limitation was further elucidated by Xu et al., who established a direct correlation between conductivity (or impedance) and microcrystalline order [131]. Using the horizontal extension length (La) and vertical stacking thickness (Lc) to quantify graphitization, they confirmed that impedance is negatively correlated with crystallite size. This mechanism explains the mechanistic inefficiency observed by Antic Gorrazzi et al.: the minimal La and Lc in medium-to-low temperature biochar represent a

lack of ordered channels for electron migration. Therefore, the fundamental barrier to the DET pathway in low-temperature biochar is not primarily surface chemistry but rather this intrinsic amorphous structure and its consequent high electrical impedance.

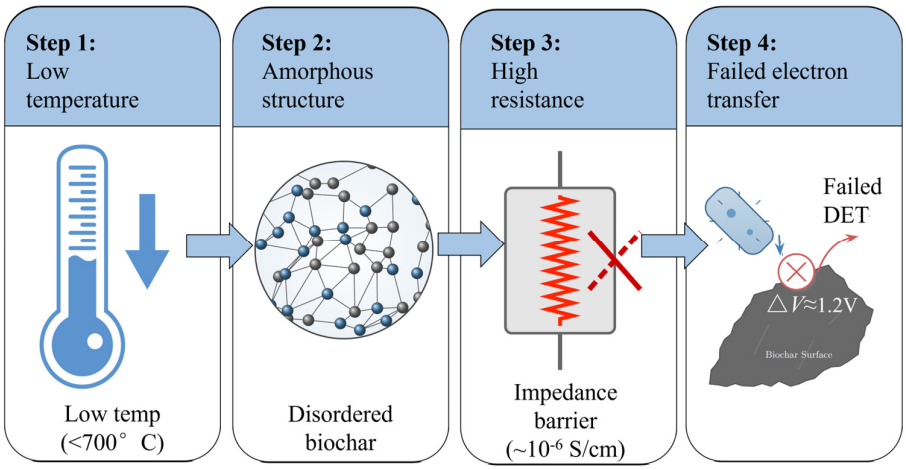


Figure 4. DET failure mechanism in biochar (<700 °C). This lack of graphitization results in high impedance (~10^{-6} S/cm), creating a prohibitive potential drop ($\Delta V \approx 1.2$ V) that physically blocks bacterial electron transfer. (Red crosses indicate blocked pathways; red arrows denote failed electron transfer).

3.6. Limitations of Classical Characterization Methods

While such elegant deductions of dynamic, multi-site mechanisms provide critical insights, directly and unambiguously verifying these complex site-switching processes remains a formidable challenge. This persistent ambiguity is fundamentally rooted in the inherent limitations of classical characterization methods, which struggle to capture the highly localized and dynamic nature of M–BC systems [132].

Macroscopically, widely used techniques such as sorption-based methods (e.g., BET) and Temperature-Programmed Reduction (TPR) predominantly reflect the bulk properties of the composites [133]. They lack the spatial resolution required to differentiate the highly interwoven active sites (e.g., carbon defects vs. metal clusters) at the solid–liquid interface. Microscopically, while HRTEM provides ultra-high spatial resolution, its extremely limited field of view often fails to represent the macroscopic reality of the bulk catalyst [134]. Furthermore, distinguishing single-atom or sub-nanometer active metal clusters against the thick, highly defective, and amorphous carbon matrix of biochar remains highly challenging, not to mention the potential structural alteration induced by high-energy electron beams during observation [135].

Beyond spatial resolution, the lack of dynamic temporal insights further obscures the identification of true active sites. Conventional ex situ spectroscopic tools, including X-ray photoelectron spectroscopy (XPS), X-ray absorption near-edge structure (XANES), and extended X-ray absorption fine structure (EXAFS), are typically conducted under ultrahigh vacuum conditions, capturing only the static "dead state" of the catalyst before or after the reaction [136]. These measurements inherently fail to disclose the dynamic structural reconstruction, valence evolution, or the aforementioned "substrate-dependent site switching" occurring in the actual aqueous catalytic environment [137]. To bridge this dynamic gap, operando spectroscopies (e.g., in situ IR, Raman) and Density Functional Theory (DFT) calculations are frequently proposed. However, their practical application in heterogeneous M-BC water-treatment systems is still far from adequate. Operando techniques face severe technical bottlenecks primarily due to the overwhelming signal interference from liquid water and the immense difficulty of designing delicate

in situ cells that mimic real hydrodynamic conditions. Meanwhile, DFT calculations are fundamentally restricted by the "material gap." The highly complex and heterogeneous nature of M–BC is often oversimplified into idealized graphene models, rendering many theoretically predicted structure-activity relationships detached from empirical reality [138–141].

4. Future Challenges and Perspectives

Given the complexity of M–BC as a "black box" and the significant challenges in excluding inherent interference, identifying active sites, and verifying non-radical mechanisms in current research, future studies must transition from empirical screening approaches to more rigorous mechanistic resolution and rational design.

4.1. Differentiate Contributions of Inherent Components and Exogenous Metals

Addressing the issues of "inherent component interference" and "precursor heterogeneity" raised in Sections 3.1 and 3.2, there is a pressing need to establish standardized control experiment protocols. Future studies should move beyond the reliance on untreated pristine biochar—particularly from high-ash precursors such as sludge—as a control. Instead, acid-washed, demineralized biochar should be adopted as a chemically defined baseline, or the specific contribution of inherent minerals (e.g., Fe, Ca, Mg) to the overall activity must be explicitly quantified. Concurrently, a "chemical fingerprint library" for biomass precursors should be established to correlate the lignin/cellulose ratio and inherent mineral content of raw materials with the graphitization degree and active site density of the final carbon material, thereby overcoming reproducibility issues caused by a lack of standardization.

4.2. Establishing a Multi–Dimensional Mechanistic Verification System

Given the limitations of chemical quenching experiments due to competitive adsorption (Section 3.4), future studies must move beyond sole reliance on scavengers like TBA and MeOH. To verify radical-based pathways more accurately, techniques such as EPR spectroscopy coupled with spin trapping should be widely adopted, as they provide direct evidence of specific radical generation without the severe interference of competitive surface adsorption [142]. Furthermore, in situ spectroscopy techniques should be prioritized, such as in situ Raman and in situ Fourier transform infrared spectroscopy (FTIR) [143]. These methods allow researchers to monitor the dynamic evolution of functional groups (e.g., C=O, C–OH) on the catalyst surface in real-time and directly capture evidence of surface-activated complexes formation, thereby mitigating the mechanistic ambiguity associated with indirect quenching methods [144]. Beyond surface functional groups, tracking the dynamic valence and structural evolution of exogenous metal sites requires moving away from static, ex situ analyses. Future multi-dimensional systems should integrate synchrotron-based operando X-ray absorption spectroscopy (XAS) to capture real-time electronic structural changes during the catalytic process. In addition to surface functional groups, tracking the dynamic valence and structural evolution of exogenous metal sites requires a transition from conventional ex situ analyses to advanced operando techniques. Specifically, synchrotron-based operando can be employed to monitor real-time electronic structural changes during the catalytic process [145]. Furthermore, in situ liquid-cell transmission electron microscopy (LC-TEM) can be utilized to overcome the limitations of standard HRTEM, enabling direct observation of active site dynamics at the solid–liquid interface [146].

Additionally, concerning the conductivity controversy (Section 3.5), conductivity should not be assumed based merely on material type. Standardized electrochemical

tests, such as open-circuit potential (OCP) and EIS, must be utilized to quantitatively evaluate charge-transfer capacity. This enables a definitive assessment of the DET pathway's feasibility and distinguishes conductive matrices from insulating carriers.

4.3. Machine Learning-Assisted Rational Design

The synthesis of M–BC involves a high-dimensional parameter space, including metal type, pyrolysis temperature, heating rate, and precursor composition, which presents challenges that are inefficient for traditional univariate optimization experimental approaches. The integration of Machine Learning (ML) algorithms is imperative to elucidate the complex, non-linear relationships between M–BC synthesis parameters and catalytic performance. By training models, the speciation of active sites (e.g., N-doping type, defect density) formed by specific precursors under specific pyrolysis conditions can be predicted, guiding targeted synthesis and circumventing inefficient trial-and-error [147,148]. Furthermore, computational models based on DFT require substantial refinement. Current calculations frequently rely on idealized graphene models, which neglect the amorphous structure and complex solvation environments characteristic of experimentally derived M–BC [149,150]. Future models must incorporate more realistic surface representations that explicitly include coexisting defects, heteroatoms, and metal species, to enable accurate simulation of electron-transfer pathways [151,152].

4.4. Standardization and Ecological Risk Management of Biomass Precursors

Although this review primarily focuses on the catalytic mechanisms of M–BC hybrids, its ultimate purpose is to inform their safe and effective application in real-world scenarios. The transition from laboratory-scale mechanistic studies to practical application faces significant hurdles regarding precursor management, specifically their heterogeneity and inherent impurities.

To guarantee practical viability and reproducibility, it is imperative to establish standardized protocols for biomass sourcing, physicochemical characterization, and processing. Furthermore, given the inherent heterogeneity of feedstocks, future research must develop comprehensive guidelines or decision-support databases that correlate specific biomass categories (e.g., agricultural residues vs. municipal sludge) with their optimal processing conditions [153,154]. Standardizing these parameters will minimize batch-to-batch variations and provide a reliable baseline for mechanistic investigations.

Furthermore, prioritizing ecological safety necessitates stringent control and pre-treatment strategies for biomass precursors [155]. While M–BC systems aim to reduce metal leaching, certain precursors (especially sewage sludge) inherently contain heavy metals, emerging contaminants, and persistent organic pollutants (POPs). Therefore, integrating optimized thermal processes with targeted chemical interventions (such as post-pyrolysis acid washing) is crucial to effectively decompose, volatilize, or firmly immobilize these hazardous constituents [156,157]. Ultimately, rigorous biotoxicity assessments of both the M–BC materials and the treated effluents are essential [158]. Establishing a closed-loop evaluation system—from precursor pre-treatment to post-reaction toxicity screening—will ensure that the "treating-waste-with-waste" strategy does not result in unintended "toxicity transfer," thereby guaranteeing that M–BC hybrids are both mechanistically efficient and ecologically benign.

5. Conclusions

M–BC is a promising and cost-effective catalyst for persulfate activation in advanced oxidation processes. Despite its proven efficacy in degrading a wide spectrum of recalcitrant organic contaminants, critical mechanistic ambiguities and practical challenges

remain. Mechanistic interpretations are frequently confounded by the intrinsic complexity of biomass precursors. Notably, the synergistic effects commonly attributed to loaded metals may partially stem from the overlooked catalytic contributions of inherent mineral impurities. This ambiguity is exacerbated by the lack of standardized experimental controls, such as demineralized biochar, and an over-reliance on chemical quenching assays, leading to pervasive contradictions regarding radical vs. non-radical pathways. Consequently, the heterogeneity of active sites hinders the establishment of universal structure–activity relationships.

Furthermore, a substantial gap exists between idealized laboratory studies and practical environmental applications. Current research predominantly focuses on synthetic wastewater, leaving a critical void in evaluating catalyst stability, dynamic deactivation, and metal leaching in complex, real-world matrices. Comprehensive techno-economic analyses and life cycle assessments (LCA) for scaled-up deployment are also conspicuously absent.

To advance M–BC technology from empirical observation to rational design, future research must prioritize standardized protocols and integrate advanced in situ characterization with theoretical simulations, which are essential to accurately delineate catalytic pathways and active sites. Resolving these fundamental and engineering bottlenecks is imperative for realizing the full potential of M–BC as a robust, scalable environmental remediation technology.

Author Contributions: Conceptualization, X.C. and L.H.; methodology, J.Y. and H.C.; writing—original draft preparation, J.Y.; writing—review and editing, X.C. and L.H.; visualization, J.Y.; supervision, X.C. and H.T.; project administration, X.C. All authors have read and agreed to the published version of the manuscript.

Funding: This research was funded by the Natural Science Foundation of Zhejiang Province (No. LZJWY22B070006).

Data Availability Statement: The original contributions presented in this study are included in the article. Further inquiries can be directed to the corresponding author.

Conflicts of Interest: The authors declare no conflicts of interest.

Abbreviations

The following abbreviations are used in this manuscript:

M–BCs	Metal–Biomass Carbon composites/hybrids
AOPs	Advanced Oxidation Processes
SR-AOPs	Sulfate Radical-based Advanced Oxidation Processes
PS	Persulfate
PMS	Peroxymonosulfate
PDS	Peroxydisulfate
BC	Biomass Carbon (or Biochar)
OFGs	Oxygen-containing Functional Groups
ROS	Reactive Oxygen Species
DET	Direct Electron Transfer
DFT	Density Functional Theory

References

1. Gopalakrishnan, G.; Jeyakumar, R.B.; Somanathan, A. Challenges and emerging trends in advanced oxidation technologies and integration of advanced oxidation processes with biological processes for wastewater treatment. *Sustainability* **2023**, *15*, 4235. [CrossRef]
2. Duan, X.; Sun, H.; Kang, J.; Wang, Y.; Indrawirawan, S.; Wang, S. Insights into Heterogeneous Catalysis of Persulfate Activation on Dimensional-Structured Nanocarbons. *ACS Catal.* **2015**, *5*, 4629–4636. [CrossRef]
3. Bermúdez, L.A.; Pascual, J.M.; Martínez, M.d.M.M.; Poyatos Capilla, J.M. Effectiveness of Advanced Oxidation Processes in Wastewater Treatment: State of the Art. *Water* **2021**, *13*, 2094. [CrossRef]
4. Satyam, S.; Patra, S. The Evolving Landscape of Advanced Oxidation Processes in Wastewater Treatment: Challenges and Recent Innovations. *Processes* **2025**, *13*, 987. [CrossRef]
5. Khan, M.A.; Mutahir, S.; Shaheen, I.; Qunhui, Y.; Bououdina, M.; Humayun, M. Recent advances over the doped g-C_3N_4 in photocatalysis: A review. *Coord. Chem. Rev.* **2025**, *522*, 216227. [CrossRef]
6. Lu, Y.; Feng, M.; Wang, Y. Enhancing the heterogeneous electro-Fenton degradation of methylene blue using sludge-derived biochar-loaded nano zero-valent iron. *J. Water Process Eng.* **2024**, *59*, 104980. [CrossRef]
7. Wang, J.; Wang, S. Activation of persulfate (PS) and peroxymonosulfate (PMS) and application for the degradation of emerging contaminants. *Chem. Eng. J.* **2018**, *334*, 1502–1517. [CrossRef]
8. Ran, M.; Du, B.; Liu, W.; Liang, Z.; Liang, L.; Zhang, Y.; Zeng, L.; Xing, M. Dynamic defects boost in-situ H_2O_2 piezocatalysis for water cleanup. *Proc. Natl. Acad. Sci. USA* **2024**, *121*, e2317435121. [CrossRef]
9. Sun, Z.; Zhang, C.; Wang, Y.; Wang, T.; Li, W.; Jiang, X.; Yang, L.; Wang, X. Zn-Schiff Base Polymer Electrocatalytic H_2O_2 Generation: Mechanistic Insights from In Situ Spectroscopy. *J. Phys. Chem. Lett.* **2025**, *16*, 9627–9635. [CrossRef]
10. Zhou, T.; Shi, C.; Wang, Y.; Wang, X.; Lei, Z.; Liu, X.; Wu, J.; Luo, F.; Wang, L. Progress of metal-loaded biochar-activated persulfate for degradation of emerging organic contaminants. *Water Sci. Technol.* **2024**, *90*, 824–843. [CrossRef]
11. Kumari, M.; Pulimi, M. Sulfate Radical-Based Degradation of Organic Pollutants: A Review on Application of Metal-Organic Frameworks as Catalysts. *ACS Omega* **2023**, *8*, 34262–34280. [CrossRef] [PubMed]
12. Hama Aziz, K.H.; Mustafa, F.S.; Karim, M.A.H.; Hama, S. Pharmaceutical pollution in the aquatic environment: Advanced oxidation processes as efficient treatment approaches: A review. *Mater. Adv.* **2025**, *6*, 3433–3454. [CrossRef]
13. Zawadzki, P. Persulfate activation by organic compounds: Advancements and challenges. *Curr. Opin. Chem. Eng.* **2022**, *37*, 100837. [CrossRef]
14. Serna-Galvis, E.A.; Mendoza-Merlano, C.; Torres-Palma, R.A.; Echavarria-Isaza, A.; Hoyos-Ayala, D.A. Materials Based on Co, Cu, and Cr as Activators of PMS for Degrading a Representative Antibiotic—The Strategy for Utilization in Water Treatment and Warnings on Metal Leaching. *Molecules* **2023**, *28*, 4536. [CrossRef]
15. Li, L.; Zhang, Y.; Yang, S.; Zhang, S.; Xu, Q.; Chen, P.; Du, Y.; Xing, Y. Cobalt-loaded cherry core biochar composite as an effective heterogeneous persulfate catalyst for bisphenol A degradation. *RSC Adv.* **2022**, *12*, 7284–7294. [CrossRef]
16. Kong, L.; Zhu, M.; Zhan, J. Nitrogen-Doped Biochar Aerogel as Efficient Peroxymonosulfate Activator for Organic Pollutant Removal. *Nanomaterials* **2025**, *15*, 865. [CrossRef]
17. Zhang, Y.; Wang, T.; Zhang, X.; Sun, Y.; Fan, G.; Song, G.; Chai, B. Porous pie-like nitrogen-doped biochar as a metal-free peroxymonosulfate activator for sulfamethoxazole degradation: Performance, DFT calculation and mechanism. *Appl. Surf. Sci.* **2024**, *647*, 158965. [CrossRef]
18. Li, Y.; Xie, Y.; Wang, X.; Wang, Y. Graphene Oxide Promoted Light Activation of Peroxymonosulfate for Highly Efficient Triphenyl Phosphate Degradation. *C* **2025**, *11*, 65. [CrossRef]
19. Yu, S.; Peng, Y.; Shao, P.; Wang, Y.; He, Y.; Ren, W.; Yang, L.; Shi, H.; Luo, X. Electron-transfer-based peroxymonosulfate activation on defect-rich carbon nanotubes: Understanding the substituent effect on the selective oxidation of phenols. *J. Hazard. Mater.* **2023**, *442*, 130108. [CrossRef]
20. Zhang, C.; Pan, R.; Wang, H.; Liu, Y.; Bai, R.; Zhang, H.; Zhang, Y.; Hu, G.; Zhou, Y.; Zhao, X. Pomelo peel biomass derived highly active advanced-oxidation-process catalyst: Complete elimination of organic pollutants. *J. Colloid Interface Sci.* **2024**, *670*, 50–60. [CrossRef]
21. Fan, X.; Lin, H.; Zhao, J.; Mao, Y.; Zhang, J.; Zhang, H. Activation of peroxymonosulfate by sewage sludge biochar-based catalyst for efficient removal of bisphenol A: Performance and mechanism. *Sep. Purif. Technol.* **2021**, *272*, 118909. [CrossRef]
22. Zhou, C.; Wang, Y. Recent progress in the conversion of biomass wastes into functional materials for value-added applications. *Sci. Technol. Adv. Mater.* **2020**, *21*, 787–804. [CrossRef] [PubMed]
23. Murtaza, G.; Ahmed, Z.; Valipour, M.; Ali, I.; Usman, M.; Iqbal, R.; Zulfiqar, U.; Rizwan, M.; Mahmood, S.; Ullah, A.; et al. Recent trends and economic significance of modified/functionalized biochars for remediation of environmental pollutants. *Sci. Rep.* **2024**, *14*, 217. [CrossRef] [PubMed]
24. Zhang, W.; Xi, R.; Li, Y.; Zhang, Y.; Wang, P.; Hu, D. Recent development of transition metal doped carbon materials derived from biomass for hydrogen evolution reaction. *Int. J. Hydrogen Energy* **2022**, *47*, 32436–32454. [CrossRef]

25. Xu, L.; Fu, B.; Sun, Y.; Jin, P.; Bai, X.; Jin, X.; Shi, X.; Wang, Y.; Nie, S. Degradation of organic pollutants by Fe/N co-doped biochar via peroxymonosulfate activation: Synthesis, performance, mechanism and its potential for practical application. *Chem. Eng. J.* **2020**, *400*, 125870. [CrossRef]
26. Xiang, W.; Yuan, L.; Chen, R.; Li, L.-P.; Liu, J.; Jin, Y. Biochar-confined Co@ Biochar-500 for peroxymonosulfate activation: Low metal leaching and efficient water disinfection. *Process Saf. Environ. Prot.* **2025**, *204*, 108043. [CrossRef]
27. Peng, X.; Wu, J.; Zhao, Z.; Wang, X.; Dai, H.; Li, Y.; Wei, Y.; Xu, G.; Hu, F. High efficiency degradation of tetracycline by peroxymonosulfate activated with Fe/NC catalysts: Performance, intermediates, stability and mechanism. *Environ. Res.* **2022**, *205*, 112538. [CrossRef]
28. Rehman, W.; Ma, Y.; khan, Z.; Laaskri, F.Z.A.; Xu, J.; Farooq, U.; Ghani, A.; Rehman, H.; Xu, Y. Biomass-derived carbon materials for batteries: Navigating challenges, structural diversities, and future perspective. *Next Mater.* **2025**, *7*, 100450. [CrossRef]
29. Yang, B.; Dai, J.; Zhao, Y.; Wu, J.; Ji, C.; Zhang, Y. Advances in preparation, application in contaminant removal, and environmental risks of biochar-based catalysts: A review. *Biochar* **2022**, *4*, 51. [CrossRef]
30. Wang, B.; Zhu, C.; Ai, D.; Fan, Z. Activation of persulfate by green nano-zero-valent iron-loaded biochar for the removal of p-nitrophenol: Performance, mechanism and variables effects. *J. Hazard. Mater.* **2021**, *417*, 126106. [CrossRef]
31. Lu, J.; Deng, X.; Huang, X.; Chen, C.; Liang, J.; Tong, Z. N-doping biochar-supported Fe-Cu bimetallic catalyst for H_2O_2 activation to remove tetracycline: Mechanism insight and performance optimization. *J. Environ. Manag.* **2025**, *395*, 127804. [CrossRef]
32. Wan, H.; Jin, R.; Tian, Z.; Qiu, X.; Zhai, S.; Niu, J.; Yang, S.; Zhao, Y. Electro-activation of peroxymonosulfate by novel Co_3O_4/sludge biochar cathode for sulfamethoxazole removal: Cobalt-mediated synergistic effect and mechanism. *Environ. Res.* **2025**, *279*, 121742. [CrossRef]
33. Tao, Y.; Sun, S.; Hu, Y.; Gong, S.; Bao, S.; Li, H.; Zhang, X.; Yuan, Z.; Wu, X. Activation of Peroxymonosulfate by Fe, O Co-Embedded Biochar for the Degradation of Tetracycline: Performance and Mechanisms. *Catalysts* **2024**, *14*, 556. [CrossRef]
34. Li, D.; Zhang, S.; Li, S.; Tang, J.; Hua, T.; Li, F. Mechanism of the application of single-atom catalyst-activated PMS/PDS to the degradation of organic pollutants in water environment: A review. *J. Clean. Prod.* **2023**, *397*, 136468. [CrossRef]
35. Hu, P.; Long, M. Cobalt-catalyzed sulfate radical-based advanced oxidation: A review on heterogeneous catalysts and applications. *Appl. Catal. B Environ.* **2016**, *181*, 103–117. [CrossRef]
36. Ren, W.; Xiong, L.; Nie, G.; Zhang, H.; Duan, X.; Wang, S. Insights into the electron-transfer regime of peroxydisulfate activation on carbon nanotubes: The role of oxygen functional groups. *Environ. Sci. Technol.* **2020**, *54*, 1267–1275. [CrossRef] [PubMed]
37. Oh, W.-D.; Dong, Z.; Lim, T.-T. Generation of sulfate radical through heterogeneous catalysis for organic contaminants removal: Current development, challenges and prospects. *Appl. Catal. B Environ.* **2016**, *194*, 169–201. [CrossRef]
38. Duan, X.; Sun, H.; Wang, S. Metal-Free Carbocatalysis in Advanced Oxidation Reactions. *Acc. Chem. Res.* **2018**, *51*, 678–687. [CrossRef]
39. Wang, Q.; Wu, Y.; Shan, Y.; Dong, W. Synergizing Surface-Bound Radicals with Singlet Oxygen to Expedite Emerging Organic Contaminant Degradation in Soil-Based Heterogeneous Surface Oxidation. *Environ. Sci. Technol.* **2025**, *59*, 22901–22913. [CrossRef]
40. Vali, S.A.; Moral-Vico, J.; Sánchez, A. Biochar-supported highly dispersed ultrasmall Cu/ZnO nanoparticles as a highly efficient novel catalyst for CO_2 hydrogenation to methanol. *Biofuel Res. J.* **2025**, *12*, 2398–2411. [CrossRef]
41. Li, T.; Ren, S.; Zhang, C.; Qiao, L.; Wu, J.; He, P.; Lin, J.; Liu, Y.; Fu, Z.; Zhu, Q.; et al. Cobalt single atom anchored on N-doped carbon nanoboxes as typical single-atom catalysts (SACs) for boosting the overall water splitting. *Chem. Eng. J.* **2023**, *458*, 141435. [CrossRef]
42. Miao, X.; Chen, X.; Wu, W.; Lin, D.; Yang, K. Topological defects strengthened nonradical oxidation performance of biochar catalyzed peroxydisulfate system. *Biochar* **2023**, *5*, 40. [CrossRef]
43. Cheng, X.; Huo, X.; Yang, B.; Li, W.; Wang, Q.; Zhang, Y. Deprivation of unpaired electrons on graphitic carbon nitride-based carbocatalysts by peroxydisulfate driving a nonradical oxidation process. *J. Clean. Prod.* **2022**, *334*, 130220. [CrossRef]
44. Wang, J.; Yu, J.; Fu, Q.; Yang, H.; Tong, Q.; Hao, Z.; Ouyang, G. Unprecedented Nonphotomediated Hole (h^+) Oxidation System Constructed from Defective Carbon Nanotubes and Superoxides. *ACS Cent. Sci.* **2021**, *7*, 355–364. [CrossRef] [PubMed]
45. Duan, X.; Sun, H.; Ao, Z.; Zhou, L.; Wang, G.; Wang, S. Unveiling the active sites of graphene-catalyzed peroxymonosulfate activation. *Carbon* **2016**, *107*, 371–378. [CrossRef]
46. Duan, X.; Sun, H.; Wang, Y.; Kang, J.; Wang, S. N-Doping-Induced Nonradical Reaction on Single-Walled Carbon Nanotubes for Catalytic Phenol Oxidation. *ACS Catal.* **2014**, *5*, 553–559. [CrossRef]
47. Gong, K.; Du, F.; Xia, Z.; Durstock, M.; Dai, L. Nitrogen-doped carbon nanotube arrays with high electrocatalytic activity for oxygen reduction. *Science* **2009**, *323*, 760–764. [CrossRef]
48. Gao, Y.; Chen, Z.; Zhu, Y.; Li, T.; Hu, C. New Insights into the Generation of Singlet Oxygen in the Metal-Free Peroxymonosulfate Activation Process: Important Role of Electron-Deficient Carbon Atoms. *Environ. Sci. Technol.* **2020**, *54*, 1232–1241. [CrossRef]
49. He, T.; Liu, Z.; Zhou, W.; Cheng, X.; He, L.; Guan, Q.; Zhou, H. Constructing the vacancies and defects by hemp stem core alkali extraction residue biochar for highly effective removal of heavy metal ions. *J. Environ. Manag.* **2022**, *323*, 116256. [CrossRef]

50. Sun, Z.-F.; Wu, S.-T.; Chen, C.; Wang, Z.-H.; Tan, J.-Y.; Zhang, Y.-T.; Wang, X.-T.; Yang, S.-S.; Xing, D.-F.; Liu, D.-M.; et al. Biochar-enhanced anaerobic digestion of sewage sludge: Comparative performance and mechanistic insights. *Water Res. X* **2025**, *29*, 100423. [CrossRef]
51. Guo, L.; Liu, D.; Han, R.; Yin, A.; Gong, G.; Li, S.; Chen, R.; Yang, J.; Liu, Z.; Zhi, K. Advances in Activation of Persulfate by Novel Carbon-Based Materials: Degradation of Emerging Contaminants, Mechanisms, and Perspectives. *Crystals* **2025**, *15*, 432. [CrossRef]
52. Guo, D.; You, S.; Li, F.; Liu, Y. Engineering carbon nanocatalysts towards efficient degradation of emerging organic contaminants via persulfate activation: A review. *Chin. Chem. Lett.* **2022**, *33*, 1–10. [CrossRef]
53. Ren, W.; Cheng, C.; Shao, P.; Luo, X.; Zhang, H.; Wang, S.; Duan, X. Origins of electron-transfer regime in persulfate-based nonradical oxidation processes. *Environ. Sci. Technol.* **2021**, *56*, 78–97.
54. Kong, F.; Liu, J.; Xiang, Z.; Fan, W.; Liu, J.; Wang, J.; Wang, Y.; Wang, L.; Xi, B. Degradation of Water Pollutants by Biochar Combined with Advanced Oxidation: A Systematic Review. *Water* **2024**, *16*, 875. [CrossRef]
55. Zhuang, Y.; Haderlein, S.B.; Hagemann, N.; Grafmüller, J.; Gogler, K.; Paul, A.; Fink, F.; Spahr, S. Activation of persulfate by biochar and iron: Role of biochar pyrolysis conditions and ash amendments. *Sep. Purif. Technol.* **2025**, *374*, 133634. [CrossRef]
56. Angin, D. Effect of pyrolysis temperature and heating rate on biochar obtained from pyrolysis of safflower seed press cake. *Bioresour. Technol.* **2013**, *128*, 593–597. [CrossRef] [PubMed]
57. Xiao, F.; Bedane, A.H.; Zhao, J.X.; Mann, M.D.; Pignatello, J.J. Thermal air oxidation changes surface and adsorptive properties of black carbon (char/biochar). *Sci. Total Environ.* **2018**, *618*, 276–283. [CrossRef] [PubMed]
58. Keiluweit, M.; Nico, P.S.; Johnson, M.G.; Kleber, M. Dynamic molecular structure of plant biomass-derived black carbon (biochar). *Environ. Sci. Technol.* **2010**, *44*, 1247–1253. [CrossRef]
59. Yang, S.; Xu, S.; Tong, J.; Ding, D.; Wang, G.; Chen, R.; Jin, P.; Wang, X.C. Overlooked role of nitrogen dopant in carbon catalysts for peroxymonosulfate activation: Intrinsic defects or extrinsic defects? *Appl. Catal. B Environ.* **2021**, *295*, 120291. [CrossRef]
60. Zhu, H.; Zhang, R.; Zhang, Z.; Tan, B.; Chen, D. Synergistic catalysis of graphitic N and carbonyl groups in N-doped biochar for peroxymonosulfate activation toward non-radical tetracycline degradation. *Colloids Surf. A Physicochem. Eng. Asp.* **2026**, *734*, 139413. [CrossRef]
61. Zhu, K.; Liu, C.; Xia, W.; Wang, Y.; He, H.; Lei, L.; Ai, Y.; Chen, W.; Liu, X. Non-radical pathway dominated degradation of organic pollutants by nitrogen-doped microtube porous graphitic carbon derived from biomass for activating peroxymonosulfate: Performance, mechanism and environmental application. *J. Colloid Interface Sci.* **2022**, *625*, 890–902. [CrossRef] [PubMed]
62. Nguyen, T.H.; Nguyen, X.H.; Do, T.G.; Nguyen, L.H. Development of biochar supported $NiFe_2O_4$ composite for peroxydisulfate (PDS) activation to effectively remove moxifloxacin from wastewater. *Chem. Eng. J. Adv.* **2023**, *16*, 100550. [CrossRef]
63. Wang, J.; Chai, Z.; Yang, S.; Du, E.; Guo, H. Insights into the electron transfer regime of permanganate activation on carbon nanomaterial reduced from carbon dioxide. *J. Hazard. Mater.* **2023**, *459*, 132094. [CrossRef] [PubMed]
64. Yan, Y.; Wei, Z.; Duan, X.; Long, M.; Spinney, R.; Dionysiou, D.D.; Xiao, R.; Alvarez, P.J.J. Merits and Limitations of Radical vs. Nonradical Pathways in Persulfate-Based Advanced Oxidation Processes. *Environ. Sci. Technol.* **2023**, *57*, 12153–12179. [CrossRef]
65. Zhou, Q.; Qin, L.; Liu, H.; Zhao, D.; Yang, M.; Sun, B.; Gao, X.; Jiang, H. Microwave assisted biomass derived carbon aerogel for highly efficient oxytetracycline hydrochloride degradation: Singlet oxygen mechanism and C vacancies accelerated electron transfer. *Chem. Eng. J.* **2024**, *487*, 150370. [CrossRef]
66. Miao, X.; Chen, X.; Wu, W.; Lin, D.; Yang, K. Intrinsic defects enhanced biochar/peroxydisulfate oxidation capacity through electron-transfer regime. *Chem. Eng. J.* **2022**, *438*, 135606. [CrossRef]
67. Tan, X.; Ding, W.; Jiang, Z.; Sun, L.; Huang, Y. Reinventing MoS_2 Co-catalytic Fenton reaction: Oxygen-incorporation mediating surface superoxide radical generation. *Nano Res.* **2021**, *15*, 1973–1982. [CrossRef]
68. Huo, Y.; Zhou, G.; Guan, Y.; Meng, X.; Yan, W.; Hu, J.; Xu, Y.; Jiang, Y.; Yin, J.; Zhang, L. Trigger Singlet Oxygen Dominant Pms Activation Via G-C3n4 Carrier Inducing Oxygen Vacancies in Zncoox for Enhanced Universality and Stability in Tc Degradation. Available online: https://ssrn.com/abstract=4616234 (accessed on 15 January 2026).
69. Liu, F.; Zhang, Y.; Wang, S.; Gong, T.; Hua, M.; Qian, J.; Pan, B. Metal-free biomass with abundant carbonyl groups as efficient catalyst for the activation of peroxymonosulfate and degradation of sulfamethoxazole. *Chem. Eng. J.* **2022**, *430*, 132767. [CrossRef]
70. Zhang, S.; Liu, F.; Chen, Q.; Jiang, S.; Pan, F.; Liu, Y. Enhanced Peroxymonosulfate Activation by a Benzoquinone-Functionalized Carbon Nanotube Filter for Micropollutant Degradation. *ACS EST Water* **2024**, *4*, 698–706. [CrossRef]
71. Bao, X.; Zhou, L.; Liu, B.; Zhang, G.; Fang, Y.; Zeng, Y. Peroxydisulfate activation by one-step pyrolysis iron-rich sludge biochar for tetracycline removal in water: Performance, mechanism and degradation pathway. *Biochar* **2025**, *7*, 87. [CrossRef]
72. Huang, L.; Zhu, W.; Wu, Y. Advancements in transition metal iron-based catalysts: Enhancing catalytic activity through electron transfer. *Catal. Sci. Technol.* **2025**, *15*, 3784–3792. [CrossRef]
73. Yun, E.-T.; Park, S.-W.; Shin, H.J.; Lee, H.; Kim, D.-W.; Lee, J. Peroxymonosulfate activation by carbon-encapsulated metal nanoparticles: Switching the primary reaction route and increasing chemical stability. *Appl. Catal. B Environ.* **2020**, *279*, 119360. [CrossRef]

74. Hu, H.; Chen, D.; Liang, Y.; Wang, W.; Lin, Y.; Xu, X.; Wang, X.; Wang, K.; Zhang, Y.; Ou, J.Z. Understanding the active sites and associated reaction pathways of metal-free carbocatalysts in persulfate activation and pollutant degradation. *Environ. Sci. Nano* **2024**, *11*, 1368–1393. [CrossRef]
75. Li, Y.; Hu, J.; Bao, Y.; Xiao, Y.; Lin, L.; Li, B.; Li, X.-Y. High-valent iron–oxo species in heterogeneous catalysis: Formation, mechanism, and reactivity for the degradation of various emerging organic contaminants. *Chem. Eng. J.* **2024**, *501*, 157490. [CrossRef]
76. Qu, X.; Alvarez, P.J.; Li, Q. Impact of sunlight and humic acid on the deposition kinetics of aqueous fullerene nanoparticles (nC_{60}). *Environ. Sci. Technol.* **2012**, *46*, 13455–13462. [CrossRef] [PubMed]
77. Wang, N.; Yang, J.; Li, S.; Ren, Z.; Xu, Q. Microenvironment modulation of single-atom sites and its applications in Fenton-like reactions. *Chem. Sci.* **2025**, *16*, 19072–19098. [CrossRef]
78. Xue, X.; Xue, N.; Ouyang, D.; Yang, L.; Wang, Y.; Zhu, H.; Aihemaiti, A.; Yin, J. Biochar-Based Single-Atom Catalyst with Fe-N_3O-C Configuration for Efficient Degradation of Organic Dyes by Peroxymonosulfate Activation. *ACS Appl. Mater. Interfaces* **2023**, *15*, 57003–57014. [CrossRef]
79. Kappler, A.; Wuestner, M.L.; Ruecker, A.; Harter, J.; Halama, M.; Behrens, S. Biochar as an Electron Shuttle between Bacteria and Fe(III) Minerals. *Environ. Sci. Technol. Lett.* **2014**, *1*, 339–344. [CrossRef]
80. Wu, Q.Y.; Yang, Z.W.; Wang, Z.W.; Wang, W.L. Oxygen doping of cobalt-single-atom coordination enhances peroxymonosulfate activation and high-valent cobalt-oxo species formation. *Proc. Natl. Acad. Sci. USA* **2023**, *120*, e2219923120. [CrossRef]
81. Zhao, Z.; Dai, H.; Nie, T.; Hu, T.; Zhou, W.; Zhang, M.; Xu, J.; Lin, D.; Zhu, L. Dynamic electronic modulation of single-atom Fe sites with p-block metal coordination enables highly selective generation of Fe(IV) = O in Fenton-like reactions. *Nat. Commun.* **2025**, *16*, 11290. [CrossRef]
82. Zhang, B.; Li, X.; Akiyama, K.; Bingham, P.A.; Kubuki, S. Elucidating the mechanistic origin of a spin state-dependent FeN x–C catalyst toward organic contaminant oxidation via peroxymonosulfate activation. *Environ. Sci. Technol.* **2021**, *56*, 1321–1330. [CrossRef] [PubMed]
83. Wang, Y.; Liu, Z.; Kang, W.; Li, T.; Wang, H. Plant Polyphenol-Driven Polymerization-Confinement Strategy toward Ultrahighly Loaded Atomically Dispersed FeCo Bimetallic Catalysts for Singlet Oxygen-Dominated Fenton-like Reactions. *ACS EST Eng.* **2024**, *4*, 2263–2273. [CrossRef]
84. Qi, J.; Yang, X.; Pan, P.Y.; Huang, T.; Yang, X.; Wang, C.C.; Liu, W. Interface Engineering of $Co(OH)_2$ Nanosheets Growing on the $KNbO_3$ Perovskite Based on Electronic Structure Modulation for Enhanced Peroxymonosulfate Activation. *Environ. Sci. Technol.* **2022**, *56*, 5200–5212. [CrossRef] [PubMed]
85. Lu, J.; Lu, Q.; Di, L.; Zhou, Y.; Zhou, Y. Iron-based biochar as efficient persulfate activation catalyst for emerging pollutants removal: A review. *Chin. Chem. Lett.* **2023**, *34*, 108357. [CrossRef]
86. Deng, Z.; Ma, Y.; Zhu, J.; Zeng, C.; Liu, Y.; Zhang, Z. Enhanced oxidation of sulfonamides by low-valent Cu-based sludge biochar activating ferrate (VI): The roles of valence-dependent activation pathways. *Appl. Catal. B Environ. Energy* **2025**, *371*, 125208. [CrossRef]
87. Magee, J.C.; Seenthia, N.I.; Wadzuk, B.; Hamidi, D.; He, K.; Blaney, L.; Xu, W. Tailored carbonaceous materials as biofilter amendments for PFAS removal in stormwater runoff. *Water Res.* **2026**, *288*, 124569. [CrossRef]
88. Ding, Y.; Dai, X.; Wu, B.; Liu, Z.; Dai, L. Targeted clean extraction of phosphorus from waste activated sludge: From a new perspective of phosphorus occurrence states to an innovative approach through acidic cation exchange resin. *Water Res.* **2022**, *215*, 118190. [CrossRef]
89. Wilk, M.; Śliz, M.; Czerwińska, K.; Gajek, M.; Kalemba-Rec, I. Improvements in dewaterability and fuel properties of hydrochars derived from hydrothermal co-carbonization of sewage sludge and organic waste. *Renew. Energy* **2024**, *227*, 120547. [CrossRef]
90. Yan, C.; Li, J.; Sun, Z.; Wang, X.; Xia, S. Mechanistic insights into removal of pollutants in adsorption and advanced oxidation processes by livestock manure derived biochar: A review. *Sep. Purif. Technol.* **2024**, *346*, 127457. [CrossRef]
91. Wang, Y.; Xu, J.; Wang, X.; Li, T.; Zhang, G.; Yan, Z.; Liu, J.; Wang, L. Biomimetic synthesis technology for preparation of Fe_3O_4-encapsulated biochar using in highly efficient peroxodisulfate activation. *Front. Chem.* **2022**, *10*, 967589. [CrossRef]
92. Huang, R.; Nicholas, S.; Wei, Z. Thermochemical Transformation of Calcium during Biomass Burning and the Effects on Postfire Aqueous Dissolution of Macronutrients. *Environ. Sci. Technol.* **2024**, *58*, 17304–17312. [CrossRef] [PubMed]
93. Kanafin, Y.N.; Turpanova, R.; Beisekova, M.; Poulopoulos, S.G. Sewage Sludge Biochar as a Persulfate Activator for Methylene Blue Degradation. *Clean Technol.* **2025**, *7*, 74. [CrossRef]
94. Liu, S.; Wang, J.; Zhang, Z.; Dou, M.; Huo, K.; Ding, G.; Zhou, Y.; Qiao, C. Persulfate activation by sludge-derived biochar for efficient degradation of 2,4-dichlorophenol: Performance and mechanism. *Environ. Sci. Pollut. Res. Int.* **2023**, *30*, 45259–45273. [CrossRef] [PubMed]
95. Li, X.; Cao, H.; Cao, Y.; Zhao, Y.; Zhang, W.; Shen, J.; Sun, Z.; Ma, F.; Gu, Q. Insights into the mechanism of persulfate activation with biochar composite loaded with Fe for 2,4-dinitrotoluene degradation. *J. Environ. Manag.* **2023**, *341*, 117955. [CrossRef]

96. Giudicianni, P.; Gargiulo, V.; Grottola, C.M.; Alfè, M.; Ferreiro, A.I.; Mendes, M.A.A.; Fagnano, M.; Ragucci, R. Inherent metal elements in biomass pyrolysis: A review. *Energy Fuels* **2021**, *35*, 5407–5478. [CrossRef]
97. Collett, C.; Mašek, O.; Razali, N.; McGregor, J. Influence of Biochar Composition and Source Material on Catalytic Performance: The Carboxylation of Glycerol with CO_2 as a Case Study. *Catalysts* **2020**, *10*, 1067. [CrossRef]
98. Li, Y.; Williams, P.T. Catalytic biochar and refuse-derived char for the steam reforming of waste plastics pyrolysis volatiles for hydrogen-rich syngas. *Ind. Eng. Chem. Res.* **2023**, *62*, 14335–14348. [CrossRef]
99. Kajita, M.; Kimura, T.; Norinaga, K.; Li, C.-Z.; Hayashi, J.-i. Catalytic and Noncatalytic Mechanisms in Steam Gasification of Char from the Pyrolysis of Biomass. *Energy Fuels* **2010**, *24*, 108–116. [CrossRef]
100. Zhang, M.; Peng, F.; Yu, J.; Liu, Z. Feedstock-Induced Changes in the Physicochemical Characteristics of Biochars Produced from Different Types of Pecan Wastes. *Forests* **2024**, *15*, 366. [CrossRef]
101. Kakkar, A.; Gurjar, R.; Kumar, S. Transforming waste to wealth: Biochar production from MSW for pollution mitigation and resource recovery. *Bulg. Chem. Commun.* **2025**, *57*, 150–168. [CrossRef]
102. Liu, T.; Li, Y.; Peng, N.; Lang, Q.; Xia, Y.; Gai, C.; Zheng, Q.; Liu, Z. Heteroatoms doped porous carbon derived from hydrothermally treated sewage sludge: Structural characterization and environmental application. *J. Environ. Manag.* **2017**, *197*, 151–158. [CrossRef] [PubMed]
103. Makinde, W.O.; Hassan, M.A.; Semida, W.M.; Pan, Y.; Guan, G.; Lopez-Salas, N.; Khalil, A.S.G. Heteroatom co-doped green pea peel-derived biochar for high-performance energy storage applications. *RSC Adv.* **2025**, *15*, 15819–15831. [CrossRef] [PubMed]
104. Gao, Y.; Gao, W.; Zhu, H.; Chen, H.; Yan, S.; Zhao, M.; Sun, H.; Zhang, J.; Zhang, S. A Review on N-Doped Biochar for Oxidative Degradation of Organic Contaminants in Wastewater by Persulfate Activation. *Int. J. Environ. Res. Public Health* **2022**, *19*, 14805. [CrossRef]
105. Fang, J.; He, F.; Yan, Z.; Wang, J.; Yu, R.; Zhou, H. Pyrite/biochar-activated peroxymonosulfate strengthens tetracycline degradation: Important roles of surface functional groups and Fe(II)/Fe(III) redox cycling. *J. Environ. Chem. Eng.* **2024**, *12*, 112923. [CrossRef]
106. Xu, M.; Wu, J.; Wang, J.; Zhou, W.; Li, Y.; Li, H. Bamboo leaf-derived biochar/iron silicate composite for an adsorption-degradation synergistic removal of ciprofloxacin. *Process Saf. Environ. Prot.* **2024**, *186*, 1183–1196. [CrossRef]
107. Wang, S.; Li, H.; Wu, M. Advances in metal/ biochar catalysts for biomass hydro-upgrading: A review. *J. Clean. Prod.* **2021**, *303*, 126825. [CrossRef]
108. Premchand, P.; Fino, D.; Demichelis, F.; Bensaid, S.; Chiaramonti, D.; O'Connell, G.; Scott, J.; Antunes, E. Synthesis of metal-free heteroatom (N, P, O, and B) doped biochar catalysts for enhanced catalytic co-pyrolysis of walnut shells and palm oil fatty acid distillate to produce high-quality bio-oil. *J. Environ. Chem. Eng.* **2024**, *12*, 113630. [CrossRef]
109. Ni, Y.; Liu, S.; Yi, W.; Ma, J.; Dong, Q.; Zhang, C. Synergistic microwave–metal interactions in polyurethane/biomass co-pyrolysis: Unraveling reaction mechanisms and product selectivity control. *Green Chem.* **2025**, *27*, 13692–13710. [CrossRef]
110. Ning, S.; Huang, S.; Yang, H.; Zhao, B.; Su, Y. Bimetal catalyst based on Fe and Co supported on Al pillared interlayer clays: Preparation, reactivity and mechanism for SCR-CH_4. *iScience* **2023**, *26*, 107432. [CrossRef]
111. Hu, Q.; Zhang, J.; Pan, Y.; Ding, K.; Xu, C.; Hou, J.; Liu, W.; Thanachayanont, C.; Lampang, T.N.; Chen, M.; et al. Oxygen-containing functional groups of biochars enhancing the oxygen release of CaO_2 and the generation of free radicals. *Process Saf. Environ. Prot.* **2025**, *198*, 107126. [CrossRef]
112. Gao, W.; Li, N.; Cheng, Z.; Yan, B.; Peng, W.; Wang, S.; Chen, G. Accelerated screening of active sites on biochar for catalysis and adsorption via multidimensional fingerprint factor descriptors. *Bioresour. Technol.* **2024**, *408*, 131156. [CrossRef] [PubMed]
113. Cui, J.; Meng, H.; Chen, Y.; Zhang, Y.; Hayat, W.; Jia, C.Q. Nitrogen/Sulfur Co-Doped Biochar for Peroxymonosulfate Activation in Paracetamol Degradation: Mechanism Insight and Toxicity Evaluation. *Catalysts* **2025**, *15*, 121. [CrossRef]
114. Liang, H.; Li, R.; Liu, T.; Li, R.; Zhu, Y.; Fang, F. Rapid Degradation of Bisphenol F Using Magnetically Separable Bimetallic Biochar Composite Activated by Peroxymonosulfate. *Molecules* **2024**, *29*, 5545. [CrossRef] [PubMed]
115. Ren, R.; Shang, X.; Song, Z.; Li, C.; Wang, Z.; Qi, F.; Ikhlaq, A.; Kumirska, J.; Maria Siedlecka, E.; Ismailova, O. Active electronic structure derived by Fe-Cl-C coordination of single-atom cathode applied in antibiotics degradation by electro-Fenton: Enhanced transformation of oxygen to hydroxyl radicals via 3-electron pathway. *Chem. Eng. J.* **2023**, *474*, 14554. [CrossRef]
116. Timilsina, A.; Lokesh, S.; Shahriar, A.; Numan, T.; Schramm, T.; Stincone, P.; Nyarko, L.K.; Dewey, C.; Boiteau, R.; Petras, D.; et al. Identifying Quinones in Complex Aqueous Environmental Media (Biochar Extracts) through Tagging with Cysteine and Cysteine-Contained Peptides and High Resolution Mass Spectrometry Analysis. *Environ. Sci. Technol.* **2024**, *58*, 16432–16443. [CrossRef]
117. Gu, J.; Song, Y.; Yang, Y.; Guan, C.; Jiang, J. Mechanical Insights into Activation of Peroxides by Quinones: Formation of Oxygen-Centered Radicals or Singlet Oxygen. *Environ. Sci. Technol.* **2022**, *56*, 8776–8783. [CrossRef]
118. Zeng, H.; Che, Y.; Yang, B.; Deng, J.; Zhang, C.; Wang, J.; Zhang, H. Differential catalytic mechanism induced by selective adsorption of pollutants in metal clusters decorated single atom catalyst mediated heterogeneous Fenton-like reaction. *J. Hazard. Mater.* **2025**, *491*, 138029. [CrossRef]

119. Guo, L.; Zhao, L.; Tang, Y.; Zhou, J.; Shi, B. Peroxydisulfate activation using Fe, Co co-doped biochar and synergistic effects on tetracycline degradation. *Chem. Eng. J.* **2023**, *452*, 139381. [CrossRef]
120. Wu, B.; Wang, Z.; Jia, Y.; Xu, N.; Liao, L.; Zhang, C.; Wang, Z.; Shan, Y.; Feng, W.; Xue, H. MoO_2-enhanced Fe-loaded biochar promotes Fe^{2+}/Fe^{3+} cycling for activation of peroxydisulfate to degrade organic pollutants. *Environ. Technol. Innov.* **2024**, *35*, 103736. [CrossRef]
121. Xiao, R.; Luo, Z.; Wei, Z.; Minakata, D.; Spinney, R.; Wacławek, S.; Zeng, W.; Tang, C. Beyond the bench: Evaluating the reliability of chemical scavengers in radical-based advanced oxidation processes. *Chin. Chem. Lett.* **2025**, *37*, 111853. [CrossRef]
122. Zhang, X.; Gang, D.D.; Lei, X.; Wang, T.; Lian, Q.; Holmes, W.E.; Fei, L.; Zappi, M.E.; Yao, H. Surface-bound hydroxyl radical-dominated degradation of sulfamethoxazole in the amorphous FeOOH/ peroxymonosulfate system: The key role of amorphous structure enhancing electron transfer. *Environ. Res.* **2022**, *214*, 113964. [CrossRef] [PubMed]
123. Wang, J.; Wang, S. Generation, Detection and Regulation Strategies of Reactive Species in Persulfate Activation Systems. *Environ. Microb. Technol.* **2026**, *1*, 8. [CrossRef]
124. Feng, Y.; Lee, P.H.; Wu, D.; Shih, K. Surface-bound sulfate radical-dominated degradation of 1,4-dioxane by alumina-supported palladium (Pd/Al_2O_3) catalyzed peroxymonosulfate. *Water Res.* **2017**, *120*, 12–21. [CrossRef] [PubMed]
125. Wang, L.; Lan, X.; Peng, W.; Wang, Z. Uncertainty and misinterpretation over identification, quantification and transformation of reactive species generated in catalytic oxidation processes: A review. *J. Hazard. Mater.* **2021**, *408*, 124436. [CrossRef]
126. Wu, J.H.; Yu, H.Q. Confronting the Mysteries of Oxidative Reactive Species in Advanced Oxidation Processes: An Elephant in the Room. *Environ. Sci. Technol.* **2024**, *58*, 18496–18507. [CrossRef]
127. Liu, Q.; Zhou, B.; Zheng, C.; Wang, D.; Ge, Y.; Fang, S. The CoO-doped carbon nanotubes enhance electronic performance and effectively activate persulfate for the degradation of sulfafurazole. *Environ. Res.* **2024**, *251*, 118646. [CrossRef]
128. Zhang, Y.; Gao, Q.; Xi, P.; Liu, C.; Wan, J.; Ma, Y. Fe/Zn co-doped carbonaceous activators for enhanced electron transfer in non-radical pathways: Harnessing differences in interfacial energy field gradients to trigger electron accumulation effects. *J. Colloid Interface Sci.* **2026**, *703*, 139087. [CrossRef]
129. Gabhi, R.; Basile, L.; Kirk, D.W.; Giorcelli, M.; Tagliaferro, A.; Jia, C.Q. Electrical conductivity of wood biochar monoliths and its dependence on pyrolysis temperature. *Biochar* **2020**, *2*, 369–378. [CrossRef]
130. Antic Gorrazzi, S.; Massazza, D.; Pedetta, A.; Silva, L.; Prados, B.; Fouga, G.; Bonanni, S. Biochar as a substitute for graphite in microbial electrochemical technologies. *RSC Sustain.* **2023**, *1*, 1200–1210. [CrossRef]
131. Xu, X.; Cao, D.; Wei, Y.; Wang, A.; Chen, G.; Wang, T.; Wang, G.; Chen, X. Impact of Graphitization Degree on the Electrochemical and Thermal Properties of Coal. *ACS Omega* **2024**, *9*, 2443–2456. [CrossRef]
132. Finzel, J.; Sanroman Gutierrez, K.M.; Hoffman, A.S.; Resasco, J.; Christopher, P.; Bare, S.R. Limits of detection for EXAFS characterization of heterogeneous single-atom catalysts. *ACS Catal.* **2023**, *13*, 6462–6473. [CrossRef]
133. de Smit, E.; de Groot, F.M.; Blume, R.; Havecker, M.; Knop-Gericke, A.; Weckhuysen, B.M. The role of Cu on the reduction behavior and surface properties of Fe-based Fischer-Tropsch catalysts. *Phys. Chem. Chem. Phys.* **2010**, *12*, 667–680. [CrossRef] [PubMed]
134. Mitchell, S.; Parés, F.; Faust Akl, D.; Collins, S.M.; Kepaptsoglou, D.M.; Ramasse, Q.M.; Garcia-Gasulla, D.; Pérez-Ramírez, J.; López, N. Automated image analysis for single-atom detection in catalytic materials by transmission electron microscopy. *J. Am. Chem. Soc.* **2022**, *144*, 8018–8029. [CrossRef] [PubMed]
135. Susi, T.; Kotakoski, J.; Arenal, R.; Kurasch, S.; Jiang, H.; Skakalova, V.; Stephan, O.; Krasheninnikov, A.V.; Kauppinen, E.I.; Kaiser, U. Atomistic description of electron beam damage in nitrogen-doped graphene and single-walled carbon nanotubes. *ACS Nano* **2012**, *6*, 8837–8846.
136. Lian, X.; Gao, J.; Ding, Y.; Liu, Y.; Chen, W. Unraveling Catalytic Reaction Mechanism by In Situ Near Ambient Pressure X-ray Photoelectron Spectroscopy. *J. Phys. Chem. Lett.* **2022**, *13*, 8264–8277. [CrossRef]
137. Fabbri, E.; Nachtegaal, M.; Binninger, T.; Cheng, X.; Kim, B.J.; Durst, J.; Bozza, F.; Graule, T.; Schaublin, R.; Wiles, L.; et al. Dynamic surface self-reconstruction is the key of highly active perovskite nano-electrocatalysts for water splitting. *Nat. Mater.* **2017**, *16*, 925–931. [CrossRef]
138. Di Liberto, G.; Barlocco, I.; Giordano, L.; Tosoni, S.; Pacchioni, G. Single-atom electrocatalysis from first principles: Current status and open challenges. *Curr. Opin. Electrochem.* **2023**, *40*, 101343. [CrossRef]
139. Sun, F.; Tang, Q.; Jiang, D.-e. Theoretical advances in understanding and designing the active sites for hydrogen evolution reaction. *ACS Catal.* **2022**, *12*, 8404–8433. [CrossRef]
140. Sarma, B.B.; Maurer, F.; Doronkin, D.E.; Grunwaldt, J.D. Design of Single-Atom Catalysts and Tracking Their Fate Using Operando and Advanced X-ray Spectroscopic Tools. *Chem. Rev.* **2023**, *123*, 379–444. [CrossRef]
141. Giulimondi, V.; Mitchell, S.; Perez-Ramirez, J. Challenges and Opportunities in Engineering the Electronic Structure of Single-Atom Catalysts. *ACS Catal.* **2023**, *13*, 2981–2997. [CrossRef]
142. Nosaka, Y.; Nosaka, A.Y. Generation and Detection of Reactive Oxygen Species in Photocatalysis. *Chem. Rev.* **2017**, *117*, 11302–11336. [CrossRef] [PubMed]

143. Xu, X.; Zhang, Y.; Chen, Y.; Liu, C.; Wang, W.; Wang, J.; Huang, H.; Feng, J.; Li, Z.; Zou, Z. Revealing *OOH key intermediates and regulating H_2O_2 photoactivation by surface relaxation of Fenton-like catalysts. *Proc. Natl. Acad. Sci. USA* **2022**, *119*, e2205562119. [CrossRef] [PubMed]
144. Groppo, E.; Rojas-Buzo, S.; Bordiga, S. The Role of In Situ/Operando IR Spectroscopy in Unraveling Adsorbate-Induced Structural Changes in Heterogeneous Catalysis. *Chem. Rev.* **2023**, *123*, 12135–12169. [CrossRef] [PubMed]
145. Timoshenko, J.; Roldan Cuenya, B. In Situ/Operando Electrocatalyst Characterization by X-ray Absorption Spectroscopy. *Chem. Rev.* **2021**, *121*, 882–961. [CrossRef]
146. Ross, F.M. Opportunities and challenges in liquid cell electron microscopy. *Science* **2015**, *350*, aaa9886. [CrossRef]
147. Fu, H.; Li, K.; Zhang, C.; Zhang, J.; Liu, J.; Chen, X.; Chen, G.; Sun, Y.; Li, S.; Ling, L. Machine-learning-assisted optimization of a single-atom coordination environment for accelerated Fenton catalysis. *ACS Nano* **2023**, *17*, 13851–13860. [CrossRef]
148. Choung, S.; Kim, M.; Moon, J.; Han, J.W. From Atomic Motif to Realistic Single Atom Catalysts through Machine Learning Interatomic Potentials. *ACS Energy Lett.* **2025**, *10*, 6288–6296. [CrossRef]
149. Han, Y.; Wei, Y.; Goswami, A.; Alexandrova, A. Uncovering the True Active Sites in Ni-N-C Catalysts for CO_2 Electroreduction. *J. Am. Chem. Soc.* **2025**, *147*, 38636–38646. [CrossRef]
150. Zhang, D.; Li, H. The potential of zero charge and solvation effects on single-atom M–N–C catalysts for oxygen electrocatalysis. *J. Mater. Chem. A* **2024**, *12*, 13742–13750. [CrossRef]
151. Yang, X.; Li, Q.; Wu, L.; Zhou, B.; Wang, Z.; Huang, Z.; Wang, M. Defect Engineering in Carbon-Based Metal-Free Catalysts: Active Sites, Reduction Mechanisms, and 3D Architectures for Sustainable 4-Nitrophenol Reduction. *Green Chem. Technol.* **2025**, *2*, 10015. [CrossRef]
152. Tran, N.V.; Liu, J.; Li, S. Dynamic Adaptation of Active Site Driven by Dual-side Adsorption in Single-Atomic Catalysts During CO_2 Electroreduction. *Angew. Chem. Int. Ed. Engl.* **2024**, *63*, e202411765. [CrossRef] [PubMed]
153. Santos, D.C.B.D.; Evaristo, R.B.W.; Dutra, R.C.; Suarez, P.A.Z.; Silveira, E.A.; Ghesti, G.F. Advancing Biochar Applications: A Review of Production Processes, Analytical Methods, Decision Criteria, and Pathways for Scalability and Certification. *Sustainability* **2025**, *17*, 2685. [CrossRef]
154. Köves, M.; Madár, V.; Ringer, M.; Kocsis, T. Overview of Traditional and Contemporary Industrial Production Technologies for Biochar along with Quality Standardization Methods. *Land* **2024**, *13*, 1388. [CrossRef]
155. Lin, F.; Xu, M.; Ramasamy, K.K.; Li, Z.; Klinger, J.L.; Schaidle, J.A.; Wang, H. Catalyst Deactivation and Its Mitigation during Catalytic Conversions of Biomass. *ACS Catal.* **2022**, *12*, 13555–13599. [CrossRef]
156. Buss, W. Pyrolysis Solves the Issue of Organic Contaminants in Sewage Sludge while Retaining Carbon—Making the Case for Sewage Sludge Treatment via Pyrolysis. *ACS Sustain. Chem. Eng.* **2021**, *9*, 10048–10053. [CrossRef]
157. Li, Z.; Yu, D.; Liu, X.; Wang, Y. The Fate of Heavy Metals and Risk Assessment of Heavy Metal in Pyrolysis Coupling with Acid Washing Treatment for Sewage Sludge. *Toxics* **2023**, *11*, 447. [CrossRef]
158. Huang, L.; Lu, H.; Wang, T. Comparative study on the mechanism and performance of antibiotics' photodegradation in seawater under the irradiation of weak visible light. *J. Water Process Eng.* **2025**, *80*, 109204. [CrossRef]

Disclaimer/Publisher's Note: The statements, opinions and data contained in all publications are solely those of the individual author(s) and contributor(s) and not of MDPI and/or the editor(s). MDPI and/or the editor(s) disclaim responsibility for any injury to people or property resulting from any ideas, methods, instructions or products referred to in the content.